NAG-1/GDF15 Exerts Anti-diabetic Effects through the Insulin Signaling Pathway

Pattawika Lertpatipanpong
Seoul National University
Jaehak Lee
Seoul National University
Thomas Eling
National Institute of Environmental Health Sciences
Seung Yon Oh
Seoul National University
Je Kyung Seong
Seoul National University
Seung Joon Baek (baeksj@snu.ac.kr)
Seoul National University

Research Article

Keywords: Nonsteroidal anti-inflammatory drug-activated gene-1 (NAG-1), anti-diabetic effects, insulin signaling pathway, high-fat diet (HFD)

Posted Date: March 1st, 2021

DOI: https://doi.org/10.21203/rs.3.rs-257216/v1

Version of Record: A version of this preprint was published at Scientific Reports on July 22nd, 2021. See the published version at https://doi.org/10.1038/s41598-021-94581-y.

Abstract

Nonsteroidal anti-inflammatory drug-activated gene-1 (NAG-1) has a role in various diseases. Here, the anti-diabetic effects of NAG-1 were evaluated using a high-fat diet (HFD)/streptozotocin (STZ)-induced diabetic mouse model. NAG-1-overexpressing transgenic (NAG-1 Tg) mice exhibited lower bodyweight and fasting blood glucose and insulin levels than wildtype (WT) mice. The homeostatic model assessment of insulin resistance scores of NAG-1 Tg mice were three times lower than those of WT mice. Hematoxylin and eosin staining demonstrated that NAG-1 Tg mice exhibited a smaller lipid droplet size in the adipose tissues, lower lipid accumulation in the hepatocytes, and larger beta cell area in the pancreas, compared to WT mice. Immunohistochemical analysis revealed downregulated expression of cleaved caspase-3, an apoptosis marker, in the beta cells of NAG-1 Tg mice. The adiponectin and leptin mRNA levels were upregulated and downregulated in NAG-1 Tg mice, respectively. Additionally, the IRS1/PI3K/AKT signaling pathway, especially *Foxo1*, which regulates gluconeogenesis in the muscle and WAT, was downregulated in NAG-1 Tg mice. Furthermore, NAG-1 overexpression promoted *As160* (AKT substrate of 160 kDa) expression in both muscles and adipocytes and the mRNA levels of the *Nlrp3* pathway members were downregulated in NAG-1 Tg mice. Our findings suggest that NAG-1 expression alleviates diabetes in mice.

Introduction

Nonsteroidal anti-inflammatory drug-activated gene 1 (NAG-1), which is also known as growth differentiation factor 15 (GDF15), macrophage inhibitory cytokine-1 (MIC-1), placental transforming growth factor β (TGF-β) (PTGFB), and prostate derived factor (PDF), is a member of the TGF-β superfamily. The signaling and function of NAG-1, which are mainly dependent on the health of the tissues and body, are associated with cell and tissue homeostasis. Previous studies have reported that patients with critical illnesses or those under stress exhibit upregulated serum NAG-1 levels[1]. In contrast, the expression of NAG-1 is downregulated under normal physiological conditions[2]. Recent studies have reported that NAG-1 is a major regulator of energy metabolism and appetite[3]. Additionally, NAG-1 is reported to contribute to the pathogenesis of various diseases, such as cardiovascular diseases, obesity, inflammation, cognitive impairment, and cancer[1]. NAG-1 exerts its effects, probably through the mature NAG-1 and pro-NAG-1 forms, which are secreted into the extracellular matrix[4–6]. In contrast to that of mature NAG-1, the biological activity of pro-NAG-1 in the extracellular matrix has not been investigated, except the nuclear translocation of intercellular pro-NAG-1 regulates the transcription of the members of the SMAD pathways[4].

The increasing prevalence of diabetes is a global health burden. Type 2 diabetes mellitus (T2DM) is characterized by persistent hyperglycemia. The major phenotypes of T2DM include dysregulated insulin response in the corresponding cells and insufficient insulin production in the pancreas. Furthermore, prolonged high blood glucose levels can lead to other complications, such as diabetic retinopathy,

diabetic neuropathy, diabetic foot, cognitive deficits and cardiovascular diseases[7]. Obesity and sedentary lifestyle are the major causes of diabetes that contribute to increased morbidity and mortality[8].

There are contradictory reports on the role of NAG-1 in diabetes. For example, a study examining the correlation between NAG-1 and beta cell function demonstrated that the serum NAG-1 levels were upregulated in the prediabetes and diabetes groups. Additionally, the upregulated serum NAG-1 levels were correlated with HbA1c, glucose, insulin, baseline and dynamic indices of insulin sensitivity[9]. These results suggest that glucose upregulates serum NAG-1 levels in patients with diabetes and that serum NAG-1 could be a potential marker to identify individuals who are at risk for developing diabetes and obesity. On the other hand, NAG-1 Tg mice exhibit decreased energy metabolism and bodyweight and improved glucose and insulin response[10]. Moreover, the administration of recombinant NAG-1 decreased food intake and bodyweight, which resulted in decreased adiposity, and improved glucose tolerance and insulin sensitivity in obese and wildtype (WT) mice[11]. Interestingly, Metformin, a first-line drug for T2DM, promotes bodyweight loss through the upregulation of NAG-1[12]. Although the role of NAG-1 in the pathogenesis of diabetes is not clear, NAG-1 expression, both mature NAG-1 and pro-NAG-1 forms, may play a role in the disease process.

The correlation between obesity-induced chronic inflammation and insulin resistance has been extensively investigated. The NLR family pyrin domain containing 3 (NLRP3) inflammasome, which plays an important role in regulating inflammatory cytokines, is associated with metabolic disorders[13]. The activation of the NLRP3 inflammasome promotes the secretion of interleukin-1β (IL-1β) and interleukin-18 (IL-18), which induce inflammation. The downregulated NLRP3 inflammasome activity in NAG-1 Tg mice may confer resistance against diet-induced obesity and improve insulin sensitivity[14]. Another study suggested that IL-1β and IL-18 are associated with obesity-associated inflammation and promote insulin resistance[15]. Thus, NLRP3 may be a novel therapeutic target to alleviate inflammasome hyperactivation in patients with diabetes.

This study aimed to elucidate the role of NAG-1 in insulin signaling, which is the major pathway that regulates cellular metabolic pathways, such as glucose and lipid metabolism. Mice were fed on high-fat diet (HFD) and administered with a low dosage of streptozotocin (STZ) to induce T2DM and the IRS1/AKT/PI3K signaling pathway was examined. The findings of this study indicated that NAG-1 regulated the insulin pathway and thus NAG-1 could be a biomarker for determining the efficacy of anti-diabetic agents.

Results

NAG-1 Tg mice exhibit decreased bodyweight and blood glucose level

It has been reported that the bodyweight of NAG-1 Tg mice is reported to be lower than that of sibling WT mice in both genetically modified and HFD-induced obesity animal models[10,16,17]. In this study, the effect of NAG-1 expression on STZ-treated mice was measured. The bodyweight of NAG-1 Tg mice was significantly lower than that of WT mice (Fig. 2A), which concurred with the findings of a previous study on non-STZ-treated mice[10]. The incremental changes in bodyweight between weeks 6 and 11 in NAG-1 Tg mice (20.65±3.27%) were markedly lower than those in WT mice (46.24±15.35%) (Fig. 2B). The blood glucose levels in NAG-1 Tg mice significantly decreased, especially after week 9, which was the timepoint at which STZ treatment was initiated (Fig. 2C). The change in blood glucose level between baseline and final week in WT mice (86.20±39.63 mg/dL) was markedly higher than that in NAG-1 Tg mice (9.60±12.85 mg/dL) (Fig. 2D). Thus, the bodyweight and blood glucose levels decreased in NAG-1 Tg mice, indicating that NAG-1 expression decrease the blood glucose level in the HFD/STZ-induced diabetic mouse model.

NAG-1 Tg mice exhibit increased insulin sensitivity

The levels of fasting blood glucose (FBS) and insulin were measured and intraperitoneal glucose tolerance test (IPGTT) and intraperitoneal insulin tolerance test (IPITT) were performed before the mice were euthanized. As shown in Fig. 3A, the FBS levels in NAG-1 Tg mice were significantly lower than those in WT mice (121.67±27.79 vs. 248.33±70.30 mg/dL; $p = 0.0216$). Compared with those in WT mice, the fasting insulin levels were significantly lower in NAG-1 Tg mice (0.28±0.03 vs. 0.65±0.19 ng/mL; $p = 0.0341$) (Fig. 3B). IPGTT and IPITT were performed to measure glucose tolerance and insulin sensitivity, respectively, in both NAG-1 Tg mice and WT mice. As shown in Fig. 3C and 3D, WT mice exhibited higher serum glucose levels than NAG-1 Tg mice during the 120-min period after glucose administration. The area under the curve (AUC) of glucose in NAG-1 Tg mice was significantly lower than that in WT mice (31,037 ± 924.55 vs. 68,877.76 ± 1,250.99; $p < 0.001$). To further examine insulin sensitivity, IPITT was performed at different time points (Figs. 3E and G). The mice were intraperitoneally administered with insulin and the blood sample was collected to measure the glucose and serum insulin levels. The glucose concentrations (Fig. 3E) significantly decreased after insulin injection, as well as after 120 min post-insulin administration, in NAG-1 Tg mice. However, the glucose concentrations were not significantly different between the two groups in the IPITT at 30- and 60-min post-insulin injection. The area under the curve (AUC) of serum glucose (Fig. 3F) in NAG-1 Tg mice was significantly lower than that in WT mice. (13,440.33 ± 645.22 vs. 19,423.00 ± 3,221.49; $p = 0.0344$). The serum insulin levels (Fig. 3G) significantly decreased at 30 min post-insulin injection. The AUC of insulin in NAG-1 Tg mice was significantly lower than that in WT mice. These results demonstrated that the NAG-1 Tg mice were more sensitive to insulin than WT mice. Further, insulin resistance and insulin sensitivity were calculated using the mathematical indices homeostatic model assessment of insulin resistance (HOMA-IR) (Fig. 3H). The HOMA-IR score (2.16 ± 0.27) in NAG-1 Tg mice was markedly lower than that in WT mice (7.00 ± 2.50), which indicated that NAG-1 overexpression increased insulin sensitivity in mice.

Effects of diabetic dyslipidemia and hepatic steatosis on HFD/STZ-induced diabetic mouse model

The results of histological staining of the liver, inguinal white adipose tissue (iWAT), epididymal white adipose tissue (eWAT), and brown adipose tissue (BAT) are shown in Fig. 4A. Compared with those in the hepatic sections of WT mice, lipid accumulation and the number of fat droplets were lower in NAG-1 Tg mice. This suggests that NAG-1 overexpression decreased hepatic steatosis. Furthermore, adipose tissue hypertrophy in NAG-1 Tg mice was lower than that in WT mice. The quantification of the histological data revealed that the size of lipid droplets in the iWAT, eWAT, and BAT of NAG-1 Tg mice was significantly smaller than that in the iWAT, eWAT, and BAT of WT mice ($p < 0.001$) (Figs. 4B–D). The number of crown-like structure (CLS), a histological hallmark of the pro-inflammatory process in the adipose tissue, of NAG-1 Tg mice was lower than that in the adipose tissue of WT mice ($p < 0.001$), which suggested that the inflammatory lesions decreased in NAG-1 Tg mice (Figs. 4E and F).

Effects of NAG-1 overexpression on pancreatic islet architecture

T2DM development is accompanied by the loss of β cells in the pancreatic islets[18]. The effect of NAG-1 overexpression on pancreatic islets was examined using hematoxylin and eosin (H&E) staining and immunohistochemistry. H&E analysis of the pancreas (Figs. 5A–C) revealed that the islet area in NAG-1 Tg mice was significantly larger than that in WT mice (32,138 ± 10,374.47 μm^2 vs. 12,459.39 ± 3,072.69 μm^2; $p = 0.004$). The mean number of beta cells per islet in NAG-1 Tg mice was significantly higher than that in WT mice (238.63 ± 61.88 cells/islet vs. 109.88 ± 37.78 cells/islet; $p = 0.002$). Immunohistochemical analysis revealed that the expression of cleaved caspase-3, a hallmark of apoptosis[19], in the pancreatic islets of NAG-1 Tg mice was lower than that in the pancreatic islets of WT mice (Fig. 5D). This indicated that NAG-1 overexpression may delays the development of T2DM and decreases apoptosis in the pancreatic islets.

Effect of NAG-1 overexpression on mRNA expression level of the insulin signaling pathway members

To confirm the NAG-1 expression in the NAG-1 Tg mice, we performed RT-PCR using tissues from muscle, iWAT and BAT. Human NAG-1 gene was only expressed in the tissues from NAG-1 Tg mice, whereas no mRNA expression of human NAG-1 gene in WT mice (Fig. 6A). Further, to elucidate the molecular mechanisms underlying the NAG-1-mediated regulation of blood glucose level, quantitative real-time polymerase chain reaction (qRT-PCR) analysis were performed to analyze the expression levels of several genes related to the insulin signaling pathway. As shown in Fig. 6B, C, and D, NAG-1 Tg mice exhibited upregulated mRNA expression levels of *Irs1*, *Glut4*, *Akt*, *Pi3k*, and *As160* in the muscle, iWAT, and BAT. These results indicate that NAG-1 may improve glucose metabolism and attenuate insulin resistance through the activation of the IRS1/AKT/PI3K signaling pathway. These results were also confirmed by measuring the mRNA expression levels of the downstream effectors of the AKT pathway, including *Gsk3b*, *Foxo1*, and *Mtor1*. The expression levels of downstream effector genes were significantly downregulated in the muscles, iWAT, and BAT of NAG-1 Tg mice. Additionally, the expression level of *Ptpn1*, a negative regulator of AKT, was downregulated in the muscles, iWAT, and BAT of NAG-1 Tg mice.

Interestingly, the expression level of *Mtor2* was significantly upregulated in the muscles but not in the iWAT and BAT. The evidence reported that *Mtorc2* in muscle tissue contributes to glucose homeostasis by positively regulating insulin-stimulated phosphorylation of the *Akt* substrate *As160* and negatively regulating basal glycogen synthase activity[20]. In contrast, *Mtorc2* in adipose tissues controls expression of the lipogenic transcription factor ChREBPβ, which increase adipose tissue de novo lipogenesis and impairs hepatic insulin sensitivity[21]. The mRNA expression level of *Pparg* was significantly upregulated in the iWAT and BAT but not in the muscles. Since the adipose tissue is the major mediator of PPARγ activity on insulin sensitivity, PPARγ activation in the mature adipocytes induces the expression of several genes involved in the insulin signaling cascade and consequently contribute to enhancing insulin sensitivity[22].

Effect of NAG-1 overexpression on the mRNA expression levels of adipocytokines

Adiponectin and leptin, which are major adipokines, are important mediators of energy homeostasis. The downregulation of adiponectin has been associated with insulin resistance, dyslipidemia, and atherosclerosis. Leptin decreases appetite, stimulates thermogenesis, enhances fatty acid oxidation, decreases glucose level, and reduces bodyweight and fat mass[23]. The effect of NAG-1 overexpression on the mRNA expression levels of adiponectin and leptin was examined in NAG-1 Tg mice. The mRNA level of adiponectin was upregulated, while that of leptin was downregulated in the muscles and iWAT of NAG-1 Tg mice. However, the mRNA level of adiponectin in the BAT was not significantly different between WT and NAG-1 Tg mice (Fig. 7).

Effect of NAG-1 overexpression on the mRNA expression level of Nlrp3 inflammasome

NLRP3 inflammasomes are involved in the secretion of inflammatory cytokines, which promote insulin resistance. Therefore, this study investigated the effects of NAG-1 overexpression on the expression of the NLRP3 inflammasome in HFD/STZ-induced diabetes mouse model. As shown in Figs. 8A–C, the mRNA expression levels of *Nlrp3* and *Casp1* in the muscles, iWAT, and BAT of NAG-1 Tg mice were significantly lower than those in the muscles, iWAT, and BAT of WT mice. Compared with those in the iWAT of WT mice, the mRNA levels of *Asc* were significantly downregulated in the iWAT but not in the muscle and BAT of NAG-1 Tg mice. Furthermore, the mRNA levels of *Il18* were significantly downregulated in the muscles and iWAT of NAG-1 Tg mice when compared with those in the muscles and iWAT of WT mice. In contrast, the mRNA levels of *Il1b* in the BAT of NAG-1 Tg were significantly lower than those in the BAT of WT mice. The expression levels of *Nlrp3* and *Casp1* were downregulated in the muscles, iWAT, and BAT of NAG-1 Tg mice. This indicated that the decreased NLRP3 inflammasome activity in NAG-1 Tg mice may alleviate diet-induced obesity and enhance insulin sensitivity in HFD/STZ mouse model.

Discussion

Mature NAG-1/GDF15 signaling in the brain exerts anti-obesity effects by regulating appetite[24] and consequently decreases bodyweight and fat mass[17]. Consistently, this anti-obesity effect was inhibited in NAG-1 knockout mice[16]. Previously, we had reported that NAG-1 is a novel therapeutic target for obesity and insulin resistance as it modulates metabolic activity by promoting the expression of key thermogenic and lipolytic genes in the BAT and WAT[10]. As NAG-1 can decrease bodyweight, it has potential applications for the prevention and treatment of obesity and hyperglycemia, which is one of the main chronic symptoms of diabetes.

The molecular mechanisms of NAG-1 in diabetes have not been elucidated. However, recent studies have suggested that treatment with NAG-1/GDF15 inhibited diabetes in 53% of non-obese diabetic mice[25]. Non-obese diabetic mice are commonly used as models to screen the therapeutic agents for type 1 diabetes because they spontaneously develop autoimmune diabetes, which mimics the diabetic condition in humans. Further evidence of the anti-diabetic role of NAG-1 was obtained from the use of metformin, an anti-diabetic drug. Treatment with metformin consistently induces weight loss in individuals with or without T2DM. Additionally, metformin is reported to upregulate the expression of NAG-1/GDF15[12], which indicated that the mechanism of action of metformin involves the induction of NAG-1 expression. However, it has been reported that the serum levels of NAG-1/GDF15 in patients with T2DM are higher than those in non-diabetic individuals[26]. Additionally, the serum levels of NAG-1/GDF15 are positively correlated with blood concentrations of glucose[27]. The mechanism underlying the upregulation of serum NAG-1/GDF15 levels in patients with diabetes has not been elucidated. One potential explanation is the presence of several forms of NAG-1 in the serum. NAG-1 is synthesized in the cytoplasm and secreted in at least two different forms of NAG-1 (pro-form and mature form). However, the molecular function of the pro-NAG-1 form in the serum has not been elucidated. The role of pro-NAG-1 in diabetes development must be examined and thus the ratio of mature form of NAG-1 to pro-form of NAG-1 could determine the progression of diabetes in patients. Furthermore, intercellular NAG-1 may also have a role in the adipose tissue, which exhibits NAG-1 expression. Previously, we had reported that pro-NAG-1 decreases SMAD activity in the nucleus through transcriptional regulation[4], which possible contribute to regulate several other mechanisms of transcriptional regulation, including micro RNA and long non-coding RNA expression. The elucidation of pro-NAG-1 function can aid in determining the role of NAG-1 in the development of diabetes.

To elucidate the mechanism involved in NAG-1/GDF15-mediated enhanced insulin sensitivity, this study investigated the insulin signaling pathway using NAG-1 Tg mouse tissues. In addition to the adipose tissue, the skeletal muscle was considered as the target tissue in which NAG-1/GDF15 was expressed. Glucose uptake by this tissue accounts for the majority of glucose disposal during the postprandial period, as well as after the challenge with exogenous insulin. The expression of GLUT4 was upregulated in the skeletal muscle of NAG-1/GDF15 Tg mice (Fig. 6), supporting the hypothesis that NAG-1/GDF15 expression in the skeletal muscle may increase systemic insulin sensitivity. The upregulated expression of *Glut4* is accompanied by the induction of the expression of *As160*, which is required for the insulin-

stimulated translocation of glucose transporter to the plasma membrane. Indeed, the expression of *Glut4* was also upregulated in the iWAT and BAT (Fig. 6).

In obesity and diabetes, PI3K/AKT is the major insulin pathway involved in physiological functions of various organs. The PI3K/AKT signaling pathway promotes lipid biosynthesis and inhibits lipolysis in the adipose tissue. *Foxo1*, which is the substrate of PI3K/AKT, regulates lipolysis by modulating the expression of adipose triglyceride lipase (ATGL). Additionally, the modulation of the PI3K/AKT signaling pathway and the downstream effectors is a potential therapeutic strategy for obesity and T2DM. However, the complex mechanism of the PI3K/AKT pathway must be elucidated in future studies. This study demonstrated that the metabolic functions of the PI3K/AKT signaling pathway in the muscle and adipose is critical for metabolism and that NAG-1 is a positive regulator of this pathway.

The mTOR protein modulates insulin signaling by regulating several downstream components[28]. The mTORC1 is a downstream effector of AKT, is involved in the conversion of BAT to WAT. Previous studies have reported that mTORC1 activation in the adipose tissue promotes the accumulation of lipids in BAT through the downregulation of brown adipocyte markers and the upregulation of WAT markers. In the skeletal muscle, *Mtorc1* regulates muscle mass by regulating protein synthesis and degradation[29]. The overactivation of mTORC1 in the muscle of obese and high-fat-fed rodents is associated with increased inhibitory phosphorylation of insulin receptor substrate-1 (IRS-1) and impaired AKT activation, which lead to impaired insulin signaling, decreased glucose uptake by the muscle, and systemic insulin resistance[30]. The findings of this study indicated that mTORC1 is downregulated in the BAT but not in the WAT, which suggested decreased conversion of BAT into WAT in NAG-1 Tg mice. This may be associated with low bodyweight and small size of droplets (Figs. 2 and 4). Moreover, *Mtorc1* was also downregulated in the muscles, which indicated decreased insulin resistance in NAG-1 Tg mice. mTORC2, a component of the mTOR complex, promotes AKT signaling through phosphorylation[31]. The knockout of mTORC2 in the muscle leads to the impairment of insulin signaling through GLUT4 translocation[20]. Additionally, the knockout of *Mtorc2* in the adipose tissues suppressed insulin-induced lipolysis, which increased the levels of circulating fatty acids and glycerol[32]. The findings of this study indicated that the expression of *Mtorc2* changes in the muscle but not in the adipose tissue of NAG-1 Tg mice. This suggested that the induction of *Mtorc2* expression in the muscles of NAG-1 Tg mice is associated with the upregulation of *As160*, which leads to the translocation of GLUT4 to the plasma membrane. Interestingly, NAG-1 regulated the expression of leptin and adiponectin in this study. Studies on animal models have revealed that leptin and adiponectin play a critical role in the prevention and control of T2DM by promoting beta cell function and survival, improving insulin sensitivity, and regulating glucose metabolism[33]. Leptin and adiponectin regulate blood glucose through several mechanisms. In this study, NAG-1 overexpression downregulated the expression of *leptin* and upregulated the expression of *adiponectin* (Fig. 7). Previous studies have reported that increased leptin levels are associated with insulin resistance and T2DM development. Additionally, increased leptin concentrations are associated with increased cardiovascular risk in patients with T2DM[34]. In this study, NAG-1 Tg mice exhibited downregulated expression of *leptin* in the WAT, BAT, and muscle, and decreased insulin resistance when compared with WT mice. Adiponectin

also contributes to improving insulin sensitivity by locally increasing GLUT4-mediated glucose uptake. However, adiponectin also inhibits BAT activation and thermogenesis in mice by suppressing *Ucp1* expression, lipolysis, and brown adipocyte recruitment[35]. This demonstrated that increased adiponectin levels are sometimes associated with metabolic dysfunction in BAT[36]. These data are consistent with the improved insulin sensitivity and increase in thermogenesis in the BAT of NAG-1 Tg mice. These results are consistent with those of our previous study, which suggested that NAG-1 mice exhibit upregulated expression of thermogenesis-related genes in the BAT[10].

NLRP3 inflammasome is the most fully characterized of the inflammasomes belongs to the nucleotide-binding oligomerization domain (NOD)–like receptor (NLR) family of pattern recognition receptors (PRRs) which found in cytosol to detecting pathogens invasion and initiating immune responses. The NLRP3 inflammasome contains 3 main components which are apoptosis-associated speck-like protein containing a CARD (ASC), proinflammatory caspase-1 and NLRP3. The activation of this inflammasome leads to secretion promotion of the proinflammatory cytokines interleukin 1β (IL-1β) and interleukin 18 (IL-18) which play roles in T2DM progression. Several studies reported that NLRP3 inflammasome and its components are crucial mechanisms that induces metabolic inflammation and insulin resistance[37].

In this study, the results show the decreasing of NLRP3 and caspase-1 mRNA expression in muscle, iWAT and BAT followed by the reduction of IL1β and IL-18 mRNA expressions in different tissues of NAG-1 Tg diabetic mice, compared to WT mice.
Similarly, in our previous research reported NAG-1 Tg mice with CHO, low-fat and high-fat diet exhibited no significant but lower expression of NLRP3 mRNA[14] and significant decline of caspase-1, ASC, IL1β and IL18 mRNA expression in WAT of NAG-1 Tg obese mice, compared with WT mice[10]. This suggests that NAG-1 Tg mice have negative correlation with NLRP3 inflammasomes which play important roles for protection against insulin resistance.

In summary, the findings of this study demonstrate that NAG-1 may inhibit diabetic development in an HFD/STZ-induced diabetic mouse model. Based on the findings of this study, we conclude that NAG-1 upregulates insulin signaling and consequently downregulates *Gsk3β*, *mTorc1*, and *Foxo1*, which may contribute to the prevention of HFD/STZ-induced diabetic mice (Fig. 9). Histological analysis revealed that NAG-1 mitigates the adverse effects of diabetes on the liver and adipose tissues. NAG-1 overexpression exerts anti-diabetic activity by increasing the pancreatic islet area and the beta cell population in the pancreas. These results also highlight the potential role of NAG-1 in the development of novel preventive approaches to manage insulin resistance.

Methods

Animals

The procedures for animal care and experiments were approved by the Institutional Animal Care and Use Committees of Seoul National University (SNU-170417-23-2).

Six-week-old male C57BL/6 mice (wildtype and NAG-1 Tg) were used in this study. The animals were housed in a temperature-controlled (21 ± 2°C) room with a 12-h dark/light cycle. The mice had free access to food and water.

All mice were maintained on HFD (60% from fat, D12492, Research Diets, Inc., New Brunswick, NJ) throughout the experimental period and the study was carried out in compliance with the ARRIVE guidelines.

Experimental design

Mice were grouped into the following two groups: WT mice and NAG-1 Tg mice (n = 5 for each group). After three weeks of maintenance on HFD, the mice were and intraperitoneally injected with STZ (40 mg/kg bodyweight; #13104, Cayman Chemical, MI, USA) after 8 h of fasting. The mice were continued to be maintained on HFD (Fig. 1). At week 10, the mice were again administered with STZ. The levels of FBG were analyzed to confirm diabetes in mice at week 11.

Measurements of bodyweight and fasting FBG and insulin levels

Bodyweight and FBG were initially measured at week 6 and monitored every week thereafter until the end of the experimental period. The FBG levels were measured using the fresh blood samples collected from the mouse tail vein with Accu-Chek® Performa (Roche Diabetes Care, Indianapolis, IN, USA). The fasting serum insulin levels were determined using the ultra-sensitive mouse insulin ELISA kit (#90080, Crystal Chem, IL, USA), following the manufacturer's instructions.

IPGTT

The mice were allowed to fast for 18 h and subjected to IPGTT on week 11. Mice were intraperitoneally injected with fresh glucose solution (2 g/kg bodyweight, A2494001, Gibco, Gaithersburg, MD, USA) and the blood glucose level was measured at 0 (baseline),15, 30, 60, and 120 min post-glucose injection using Accu-Chek® Performa. The AUC value of insulin was calculated using GraphPad Prism software (GraphPad Prism 8 Software Inc., San Diego, CA, USA).

IPITT

At week 12, the mice were allowed to fast for 6 h before the experiment. The serum glucose and insulin levels were measured using Accu-Chek® Performa at baseline (0 min) and after intraperitoneal injection of insulin (0.75 U/kg bodyweight) (I0516, Sigma-Aldrich, St. Louis, MO, USA). The blood glucose levels

and serum insulin levels were also determined at 15, 30, 60, and 120 min post-injection. Insulin resistance was calculated using the following formula: HOMA-IR index = glucose level × (serum insulin level/22.5)

Histological analysis

The pancreas, liver, muscle, iWAT, eWAT, and BAT were fixed with paraformaldehyde and subjected to H&E staining. The tissues were fixed in 10% neutral formalin, embedded in paraffin, sectioned (thickness: 5 μm), and stained with H&E. The images were captured using Panoramic SCAN (3DHISTECH, Budapest, Hungary).

Immunohistochemistry

The tissue blocks were fixed in 10% formalin, embedded in paraffin, sectioned to 5-μm-thick sections. The sections were incubated in citrate buffer for 1 min in a microwave (Immunobioscience, Mukilteo, WA, USA) to retrieve the antigens. Endogenous peroxidase activity was blocked using 0.3% hydrogen peroxide (Sigma-Aldrich, St. Louis, MO, USA) in phosphate-buffered saline for 1 h at room temperature. Immunoreactivity was detected using an ultra-sensitive ABC staining kit (Thermo Scientific, Rockford, IL, USA), following the manufacturer's instructions. The sections were incubated with rabbit polyclonal anti-cleaved caspase-3 (#9661S, Cell Signaling Technology, Beverly, MA, USA) antibody at 4°C overnight. The negative control samples were incubated with secondary antibodies but not primary antibody. The sections were incubated with 3,3'-diaminobenzidine tetrahydrochloride (DAB) substrate (ImmPACT® DAB kit, VECTOR Laboratory, Burlingame, CA, USA) at room temperature for 45 s and counterstained with hematoxylin (VECTOR Laboratory, Burlingame, CA, USA) for 30 s. Coverslip-mounted sections were observed using the Panoramic SCAN slide scanner.

Reverse transcription polymerase chain reaction (RT-PCR)

Total RNA was extracted from tissues using the RNeasy mini kit (QIAGEN, Hilden, Germany), following the manufacturer' s instructions. The 1 μg of RNA was reverse transcribed using Verso cDNA Synthesis Kit (Thermo Fisher Scientific, Waltham, MA, USA). Following by amplifying DNA by PCR using MiniAmp Plus Thermal Cycler (A37835, Applied Biosystems, Marsiling Industrial Estate, Singapore) with GoTaq® Green PCR Master Mix (Promega, Madison, WI, USA). The primers are human *NAG-1* (F: 5'-CTCCAGATTCCGAGAGTTGC-3' and R: 5'-AGAGATACGCAGGTGCAGGT-3') and mouse *β-actin* (F: 5'-GGCTGTATTCCCCTCCATCG-3' and R: 5'-CCAGTTGGTAACAATGCCATGT-3'). The thermal cycling conditions were as follows: initial denaturation at 94°C for 2 min, followed by 40 cycles of 94°C for 30 s, 52°C for 30 s, and 72°C for 1 min, then final extension at 72°C for 5 min. The products were electrophoresed on 1.5% agarose gel and were visualized under UV light using Alliance Q9 mini (Cambridge, UK).

Quantitative reverse transcription polymerase chain reaction (qRT-PCR)

Total RNA was extracted from tissues using the RNeasy mini kit (QIAGEN, Hilden, Germany), following the manufacturer's instructions. RNA (1 µg) was reverse transcribe into cDNA using the first strand cDNA synthesis kit (K1612, Thermo Scientific™, Waltham, MA, USA) in a MiniAmp Plus Thermal Cycler (A37835, Applied Biosystems, Marsiling Industrial Estate, Singapore). The primers are used for qRT-PCR analysis are shown in Table 1. The relative level of each RNA was measured using qRT-PCR with SYBR Green reagents (PowerUp™ SYBR™ Green Master Mix, A25741, Applied Biosystems, Thermo Scientific™) in QuantStudio™ 1 real-time PCR system (Applied Biosystems, Marsiling Industrial Estate, Singapore). The expression level of the target gene was normalized to that of *Gapdh* (housekeeping gene). The relative gene expression was calculated using the comparative Ct ($2^{-\Delta\Delta Ct}$) method.

Table 1
Real-time PCR primers used in this study.

	Forward primer (5'->3')	Reverse primer (5'->3')
Adiponectin	ATCTGGAGGTGGGAGACCAA	GGGCTATGGGTAGTTGCAGT
Leptin	AGGTAGGGATGGGTAGAGCC	GTGTGCTGCTTGGGAGTTTC
GLUT4	GGTGTGGTCAATACGGTCTTCAC	AGCAGAGCCACGGTCATCAAGA
PI3K	CAAACCACCCAAGCCCACTACT	CCATCAGCAGTGTCTCGGAGTT
Ptpn1	GCGCTTCTCCTACCTGGCTGTCAT	ACGTGCTCGGGTGGAAGGTCTA
IRS-1	TGTCACCCAGTGGTAGTTGCTC	CTCTCAACAGGAGGTTTGGCATG
AKT	GGACTACTTGCACTCCGAGAAG	CATAGTGGCACCGTCCTTGATC
GSK3β	CATAGTGGCACCGTCCTTGATC	CCAACTGATCCACACCACTGTC
PPARγ	GTACTGTCGGTTTCAGAAGTGCC	ATCTCCGCCAACAGCTTCTCCT
FOXO1	CTACGAGTGGATGGTGAAGAGC	CCAGTTCCTTCATTCTGCACTCG
AS160	GCCAACAGTCTTGCCTCAGAGA	CGTCTTCGGAACTGTGGAGAGT
mTORC1	CTTCCTATCCGTCTTGGCAGAC	CTCCAGACAGATGGCAATCAGG
mTORC2	CAGTGTGAGGTCCTTTCCATCC	GCCATAGATGCTTGCGACTGTG
NLRP3	TGCTCTTCACTGCTATCAAGCCCT	ACAAGCCTTTGCTCCAGACCCTAT
IL-18	TGGTTCCATGCTTTCTGGACTCCT	TTCCTGGGCCAAGAGGAAGTGATT
IL-1β	TGGACCTTCCAGGATGAGGACA	GTTCATCTCGGAGCCTGTAGTG
ASC	CTGCTCAGAGTACAGCCAGAAC	CTGTCCTTCAGTCAGCACACTG
Caspase-1	GGCACATTTCCAGGACTGACTG	GCAAGACGTGTACGAGTGGTTG
GAPDH	CATCACTGCCACCCAGAAGACTG	CATCACTGCCACCCAGAAGACTG

Statistical analysis

Data processing and analysis were performed using GraphPad Prism 8.0.1. All experimental data are represented as the mean ± standard error of the mean for parametric data. The means between two groups were analyzed using the Student's *t*-test. The data of NAG-1 Tg mice were compared with those of controls (WT mice). The differences were considered significant at *$p < 0.05$, **$p < 0.01$, or ***$p < 0.001$.

Declarations

Acknowledgements

This work was supported by the Research Institute for Veterinary Science, the BK21 PLUS Program for Creative Veterinary Science Research Center, Seoul National University, and the National Research Foundation of Korea (NRF) grant funded by the Korean government (NRF-2018R1A2B2002923) to SJB. This research was also partially supported by the R&D Project for Korea Mouse Phenotyping Center (2013M3A9D5072550) of the National Research Foundation funded by the Ministry of Science and ICT to JKS.

Author contributions

Conceptualization: P.L., T.E., and S.J.B.; Investigation: P.L., J.L., S.Y.O., and S.J.B. Resources: T.E., and J.K.S. Writing—Original Draft: P.L and S.J.B.; Writing—Review & Editing: P.L., J.L., T.E., and S.J.B.; Funding Acquisition: S.J.B.

Conflict of interest

The authors declare no conflict of interest.

Availability of materials and data

All raw and processed data for this study are provided as a supplementary file.

References

1. Baek, S. J. & Eling, T. Growth differentiation factor 15 (GDF15): A survival protein with therapeutic potential in metabolic diseases. *Pharmacol Ther.* **198**, 46–58 https://doi.org/10.1016/j.pharmthera.2019.02.008 (2019).
2. Buendgens, L. *et al.* Growth Differentiation Factor-15 Is a Predictor of Mortality in Critically Ill Patients with Sepsis. *Dis Markers.* **2017**, 5271203–5271203 https://doi.org/10.1155/2017/5271203 (2017).
3. Yang, L. *et al.* GFRAL is the receptor for GDF15 and is required for the anti-obesity effects of the ligand. *Nat Med.* **23**, 1158–1166 https://doi.org/10.1038/nm.4394 (2017).
4. Min, K. W. *et al.* NAG-1/GDF15 accumulates in the nucleus and modulates transcriptional regulation of the Smad pathway. *Oncogene.* **35**, 377–388 https://doi.org/10.1038/onc.2015.95 (2016).
5. Lee, J., Kim, I., Yoo, E. & Baek, S. J. Competitive inhibition by NAG-1/GDF-15 NLS peptide enhances its anti-cancer activity. *Biochem Biophys Res Commun.* **519**, 29–34 https://doi.org/10.1016/j.bbrc.2019.08.090 (2019).
6. Li, J. J. *et al.* Growth Differentiation Factor 15 Maturation Requires Proteolytic Cleavage by PCSK3, -5, and – 6. *Molecular and Cellular Biology.* **38**, https://doi.org/10.1128/mcb.00249-18 (2018).

7. Zhang, Z. Y. *et al.* Molecular Mechanisms of Glucose Fluctuations on Diabetic Complications. *Frontiers in Endocrinology.* **10**, https://doi.org/10.3389/fendo.2019.00640 (2019).
8. Hruby, A. & Hu, F. B. The Epidemiology of Obesity: A Big Picture. *Pharmacoeconomics.* **33**, 673–689 https://doi.org/10.1007/s40273-014-0243-x (2015).
9. Schernthaner-Reiter, M. H. *et al.* GDF15 reflects beta cell function in obese patients independently of the grade of impairment of glucose metabolism. *Nutrition, Metabolism and Cardiovascular Diseases.* **29**, 334–342 https://doi.org/10.1016/j.numecd.2018.12.008 (2019).
10. Chrysovergis, K. *et al.* NAG-1/GDF-15 prevents obesity by increasing thermogenesis, lipolysis and oxidative metabolism. *Int J Obes (Lond).* **38**, 1555–1564 https://doi.org/10.1038/ijo.2014.27 (2014).
11. Tsai, V. W. W., Husaini, Y., Sainsbury, A., Brown, D. A. & Breit, S. N. The MIC-1/GDF15-GFRAL Pathway in Energy Homeostasis: Implications for Obesity, Cachexia, and Other Associated Diseases. *Cell Metabol.* **28**, 353–368 https://doi.org/10.1016/j.cmet.2018.07.018 (2018).
12. Coll, A. P. *et al.* GDF15 mediates the effects of metformin on body weight and energy balance. *Nature.* **578**, 444–448 https://doi.org/10.1038/s41586-019-1911-y (2020).
13. Stienstra, R. *et al.* Inflammasome is a central player in the induction of obesity and insulin resistance. *Proc Natl Acad Sci U S A.* **108**, 15324–15329 https://doi.org/10.1073/pnas.1100255108 (2011).
14. Wang, X. *et al.* hNAG-1 increases lifespan by regulating energy metabolism and insulin/IGF-1/mTOR signaling. *Aging.* **6**, 690–704 https://doi.org/10.18632/aging.100687 (2014).
15. Ballak, D. B., Stienstra, R., Tack, C. J., Dinarello, C. A. & van Diepen, J. A. IL-1 family members in the pathogenesis and treatment of metabolic disease: Focus on adipose tissue inflammation and insulin resistance. *Cytokine.* **75**, 280–290 https://doi.org/10.1016/j.cyto.2015.05.005 (2015).
16. Tran, T., Yang, J., Gardner, J. & Xiong, Y. GDF15 deficiency promotes high fat diet-induced obesity in mice. *PLOS ONE.* **13**, e0201584 https://doi.org/10.1371/journal.pone.0201584 (2018).
17. Baek, S. J. *et al.* Nonsteroidal anti-inflammatory drug-activated gene-1 over expression in transgenic mice suppresses intestinal neoplasia. *Gastroenterology.* **131**, 1553–1560 https://doi.org/10.1053/j.gastro.2006.09.015 (2006).
18. Spijker, H. S. *et al.* Loss of β-Cell Identity Occurs in Type 2 Diabetes and Is Associated With Islet Amyloid Deposits. *Diabetes.* **64**, 2928 https://doi.org/10.2337/db14-1752 (2015).
19. REDDY, S., BRADLEY, J. & ROSS, J. M. Immunolocalization of Caspase-3 in Pancreatic Islets of NOD Mice during Cyclophosphamide-Accelerated Diabetes. *Annals of the New York Academy of Sciences.* **1005**, 192–195 https://doi.org/10.1196/annals.1288.025 (2003).
20. Kumar, A. *et al.* Muscle-specific deletion of rictor impairs insulin-stimulated glucose transport and enhances Basal glycogen synthase activity. *Mol Cell Biol.* **28**, 61–70 https://doi.org/10.1128/mcb.01405-07 (2008).
21. Tang, Y. *et al.* Adipose tissue mTORC2 regulates ChREBP-driven de novo lipogenesis and hepatic glucose metabolism. *Nature Communications.* **7**, 11365 https://doi.org/10.1038/ncomms11365 (2016).

22. Leonardini, A., Laviola, L., Perrini, S., Natalicchio, A. & Giorgino, F. Cross-Talk between PPARγ and Insulin Signaling and Modulation of Insulin Sensitivity. PPAR Research 2009, 818945, doi:10.1155/2009/818945 (2009).
23. Yadav, A., Kataria, M. A., Saini, V. & Yadav, A. Role of leptin and adiponectin in insulin resistance. *Clin. Chim. Acta.* **417**, 80–84 https://doi.org/10.1016/j.cca.2012.12.007 (2013).
24. Emmerson, P. J. *et al.* The metabolic effects of GDF15 are mediated by the orphan receptor GFRAL. *Nat Med.* **23**, 1215–1219 https://doi.org/10.1038/nm.4393 (2017).
25. Patel, S. *et al.* GDF15 Provides an Endocrine Signal of Nutritional Stress in Mice and Humans. *Cell Metabol.* **29**, 707–718708 https://doi.org/10.1016/j.cmet.2018.12.016 (2019).
26. Hong, J. H. *et al.* GDF15 Is a Novel Biomarker for Impaired Fasting Glucose. *Diabetes & metabolism journal.* **38**, 472–479 https://doi.org/10.4093/dmj.2014.38.6.472 (2014).
27. Bao, X. *et al.* Growth differentiation factor 15 is positively associated with incidence of diabetes mellitus: the Malmö Diet and Cancer-Cardiovascular Cohort. *Diabetologia.* **62**, 78–86 https://doi.org/10.1007/s00125-018-4751-7 (2019).
28. Yoon, M. S. The Role of Mammalian Target of Rapamycin (mTOR) in Insulin Signaling. *Nutrients.* **9**, https://doi.org/10.3390/nu9111176 (2017).
29. Laplante, M. & Sabatini, D. M. mTOR signaling in growth control and disease. *Cell.* **149**, 274–293 https://doi.org/10.1016/j.cell.2012.03.017 (2012).
30. Khamzina, L., Veilleux, A., Bergeron, S. & Marette, A. Increased activation of the mammalian target of rapamycin pathway in liver and skeletal muscle of obese rats: possible involvement in obesity-linked insulin resistance. *Endocrinology.* **146**, 1473–1481 https://doi.org/10.1210/en.2004-0921 (2005).
31. Oh, W. J. *et al.* mTORC2 can associate with ribosomes to promote cotranslational phosphorylation and stability of nascent Akt polypeptide. *Embo j.* **29**, 3939–3951 https://doi.org/10.1038/emboj.2010.271 (2010).
32. Kumar, A. *et al.* Fat cell-specific ablation of rictor in mice impairs insulin-regulated fat cell and whole-body glucose and lipid metabolism. *Diabetes.* **59**, 1397–1406 https://doi.org/10.2337/db09-1061 (2010).
33. Bortolotto, L. F. B. *et al.* Cytotoxicity of trans-chalcone and licochalcone A against breast cancer cells is due to apoptosis induction and cell cycle arrest. *Biomed. Pharmacother.* **85**, 425–433 https://doi.org/10.1016/j.biopha.2016.11.047 (2017).
34. Rodríguez, A. J., Vdos, N., Mastronardi, S., Neeman, C. A., Paz-Filho, G. J. & T. & Association between circulating adipocytokine concentrations and microvascular complications in patients with type 2 diabetes mellitus: A systematic review and meta-analysis of controlled cross-sectional studies. *J Diabetes Complications.* **30**, 357–367 https://doi.org/10.1016/j.jdiacomp.2015.11.004 (2016).
35. Qiao, L. *et al.* Adiponectin reduces thermogenesis by inhibiting brown adipose tissue activation in mice. *Diabetologia.* **57**, 1027–1036 https://doi.org/10.1007/s00125-014-3180-5 (2014).
36. CHANCLON, B., BAUZA-THORBRUGGE, M. & WERNSTEDT-ASTERHOLM, I. BENRICK, A. & 1709-P: Increased Adiponectin Levels Are Associated with Impaired Brown Adipose Tissue in Mice. **69**,1709-P,

doi:10.2337/db20-1709-P %J Diabetes (2020).

37. Zheng, D., Liwinski, T. & Elinav, E. Inflammasome activation and regulation: toward a better understanding of complex mechanisms. *Cell Discovery.* **6**, 36 https://doi.org/10.1038/s41421-020-0167-x (2020).

Figures

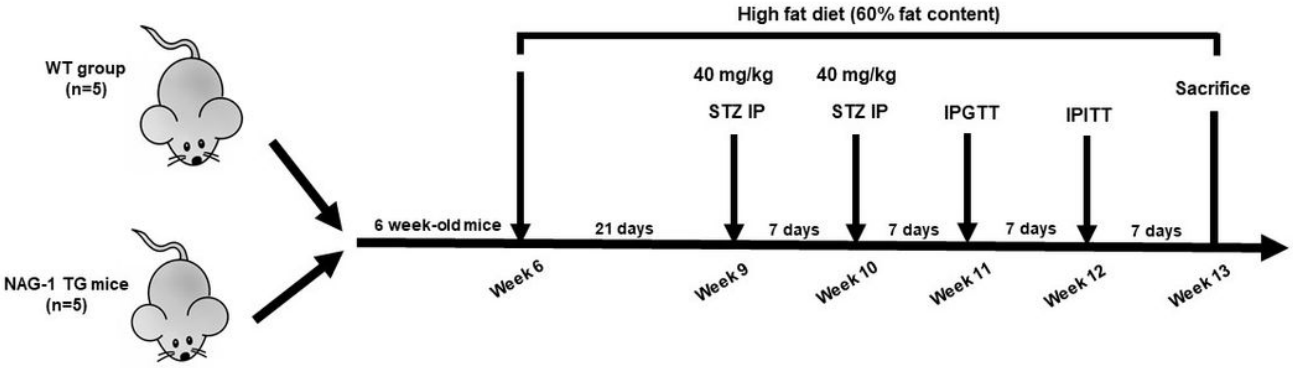

Figure1. Lertpatipanpong et al.,

Figure 1

Schematic diagram representing the timeline for experiments using the diabetes mouse model. NAG-1-overexpressing transgenic (n=5) and wildtype (n=5) male mice were fed with high-fat diet throughout the experiment. The mice were administered with streptozotocin at weeks 9 and 10. Individual mice with blood sugar levels of >200 mg/dL were considered to be animals with type 2 diabetic mellitus.

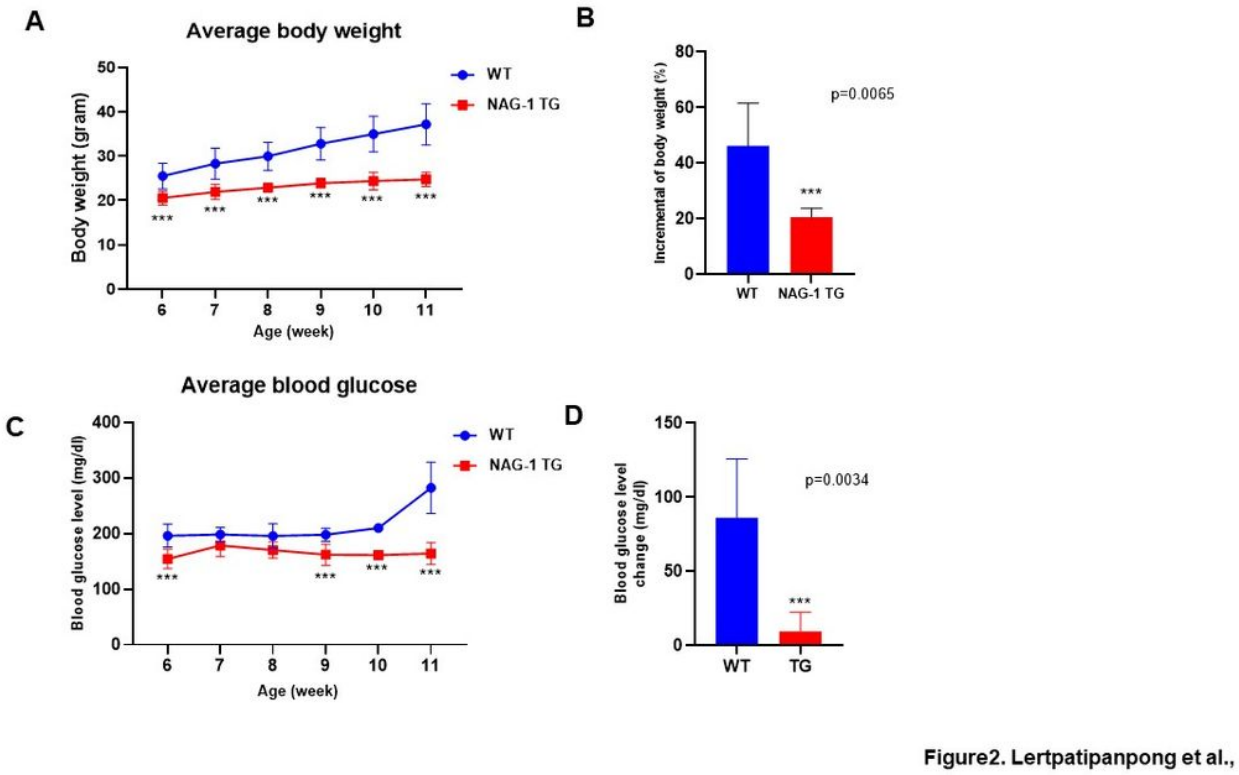

Figure2. Lertpatipanpong et al.,

Figure 2

Effects of NAG-1 on bodyweight and glucose level in high-fat diet/streptozotocin-induced diabetes mouse model. (A) Bodyweight, (B) change in bodyweight, (C) blood glucose level, and (D) change in blood glucose level. Data are presented as mean ± standard error, ***p<0.01, compared with the wildtype group. n=5 for all experiments.

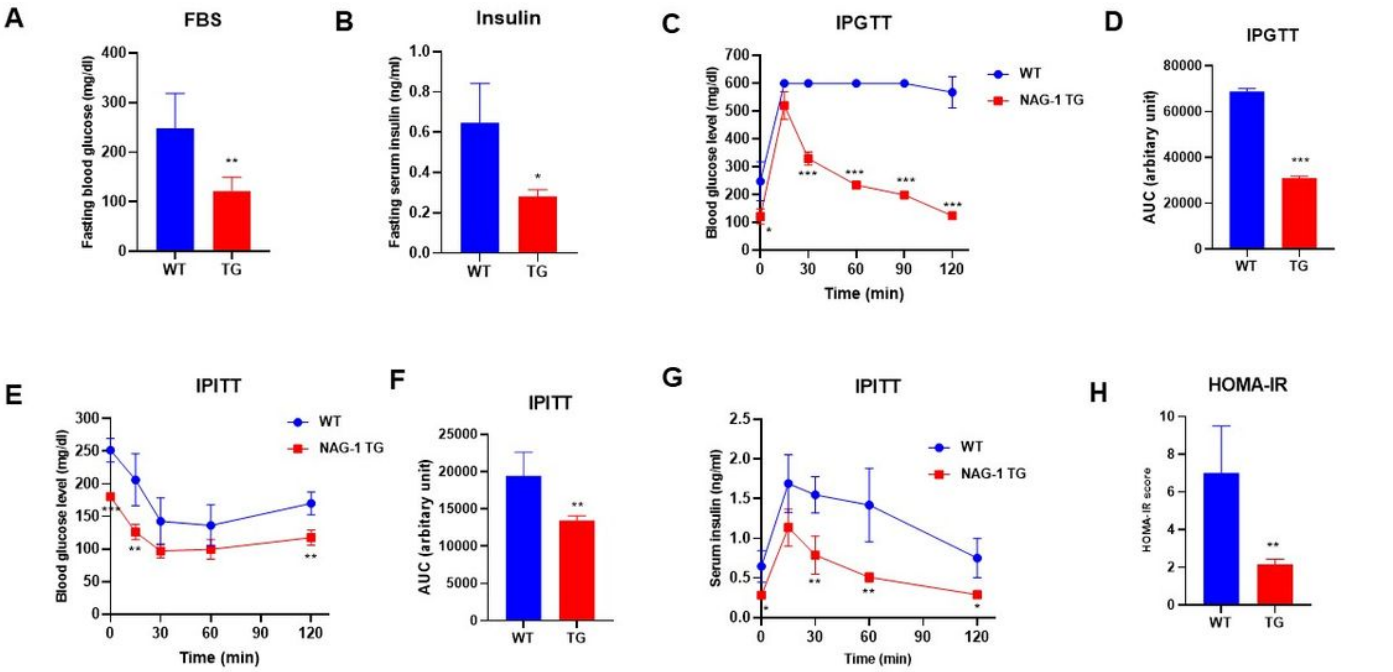

Figure3. Lertpatipanpong et al.,

Figure 3

Anti-diabetic effect of NAG-1 in high-fat diet/streptozotocin-induced diabetes mouse model. Mice were allowed to fast for 6 h before the blood sample was collected. (A) Fasting blood glucose level and (B) fasting insulin level. (C) Fasting blood glucose levels at the indicated time points in the intraperitoneal glucose tolerance test. Mice were allowed to fast for 18 h before the administration of glucose (2 g/kg bodyweight). The blood glucose levels were measured at 0, 15, 30, 60, 90, and 120 min post-glucose injection. (D) The area under the curve of glucose. (E) Fasting blood glucose levels at the indicated time point in the intraperitoneal insulin tolerance test (IPITT). Mice were allowed to fast for 6 h before the intraperitoneal administration of insulin (0.75 U/kg bodyweight). The blood samples were collected to measure the serum glucose and insulin levels at 0, 15, 30, 60, and 120 min post-insulin injection. (F) The area under the curve of glucose. (G) Serum insulin levels at the indicated time points in the IPITT. (H) Homeostatic model assessment of insulin resistance scores. Data are presented as mean ± standard error of mean. *p<0.05, **p<0.01, and ***p<0.001, compared with the wildtype group. (n=3–5)

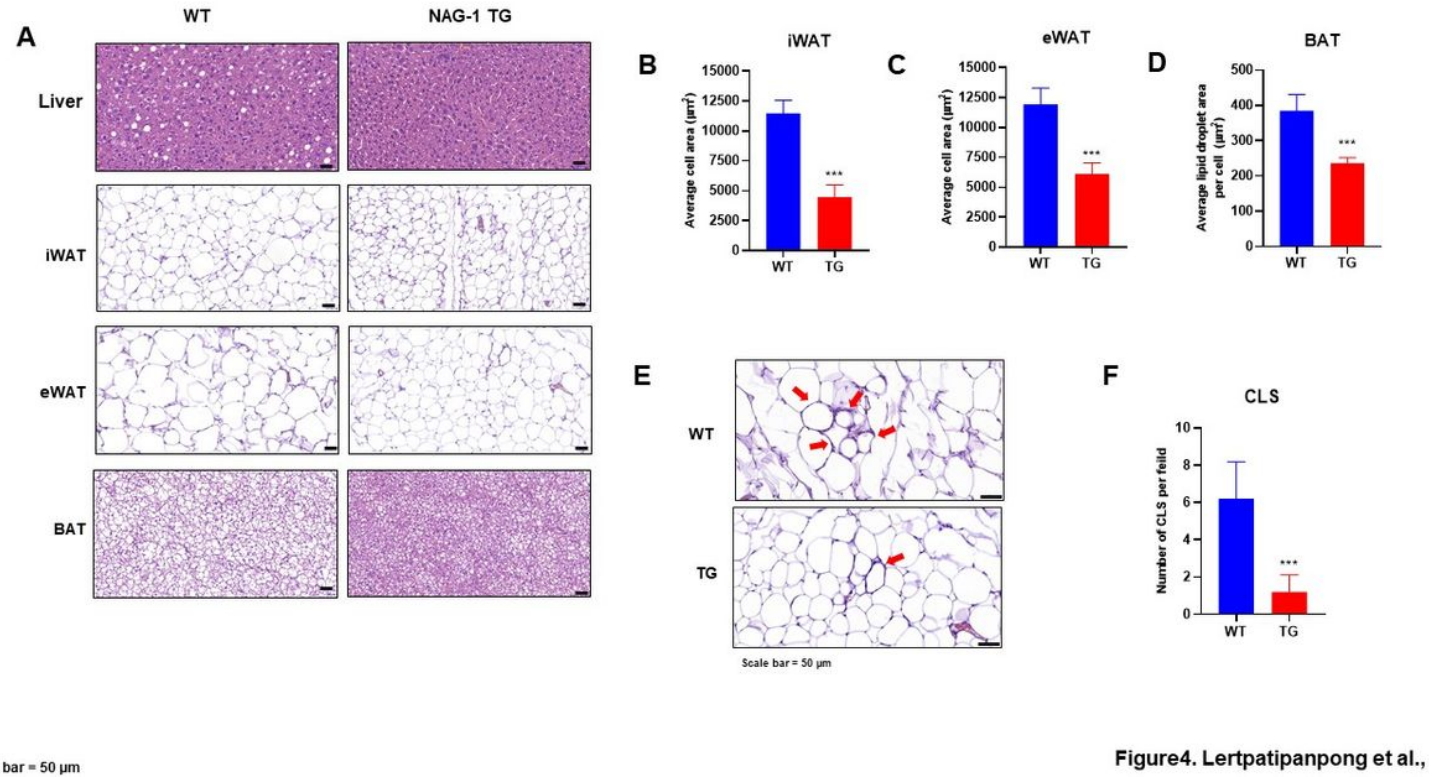

Figure 4

NAG-1 overexpression attenuated high-fat diet/streptozotocin-induced diabetic dyslipidemia and hepatic steatosis in mice. The mice were sacrificed and the liver, inguinal white adipose tissue (iWAT), epididymal white adipose tissue (eWAT), and brown adipose tissue (BAT) were excised and fixed with 4% paraformaldehyde for 24 h. The tissue sections were prepared and stained with hematoxylin and eosin (H&E). The sections were examined under a light microscope. (A) Representative image of the H&E-stained section of the liver, iWAT, eWAT, and BAT. Scale bar = 50 μm. (B, C, and D) Average lipid droplet area in the iWAT, eWAT, and BAT. (E) Histological staining of crown-like structure (CLS). Scale bar = 50 μm, (F) Number of CLS per field. (10 fields per group). Data are presented as mean ± standard error of mean. *p<0.05 and ***p<0.001, compared with the control group.

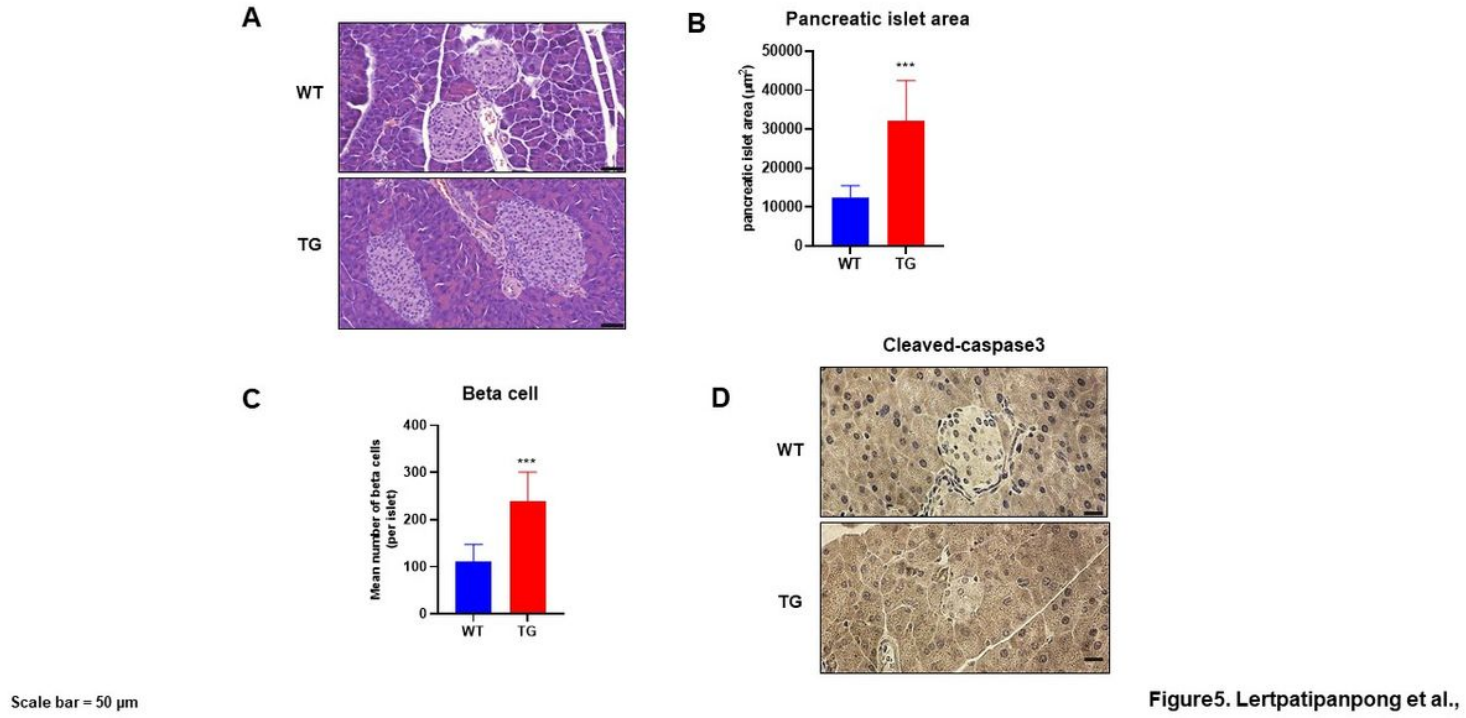

Figure 5

Pancreatic islet architecture. The mice were sacrificed and the excised pancreas was fixed with 4% paraformaldehyde for 24 h. The pancreatic sections were prepared and stained with hematoxylin and eosin (H&E) or anti-cleaved caspase-3 antibody. The sections were observed under a light microscope. (A) Representative images of H&E-stained pancreatic sections from different groups. Scale bars=50 μm. (B and C) Pancreatic islet area and beta cell number were measured as described in the methods section. Data are represented as mean ± standard error of mean. ***p < 0.01. (D) Immunohistochemical analysis of cleaved caspase-3 in the pancreas islets. Scale bars=50 μm.

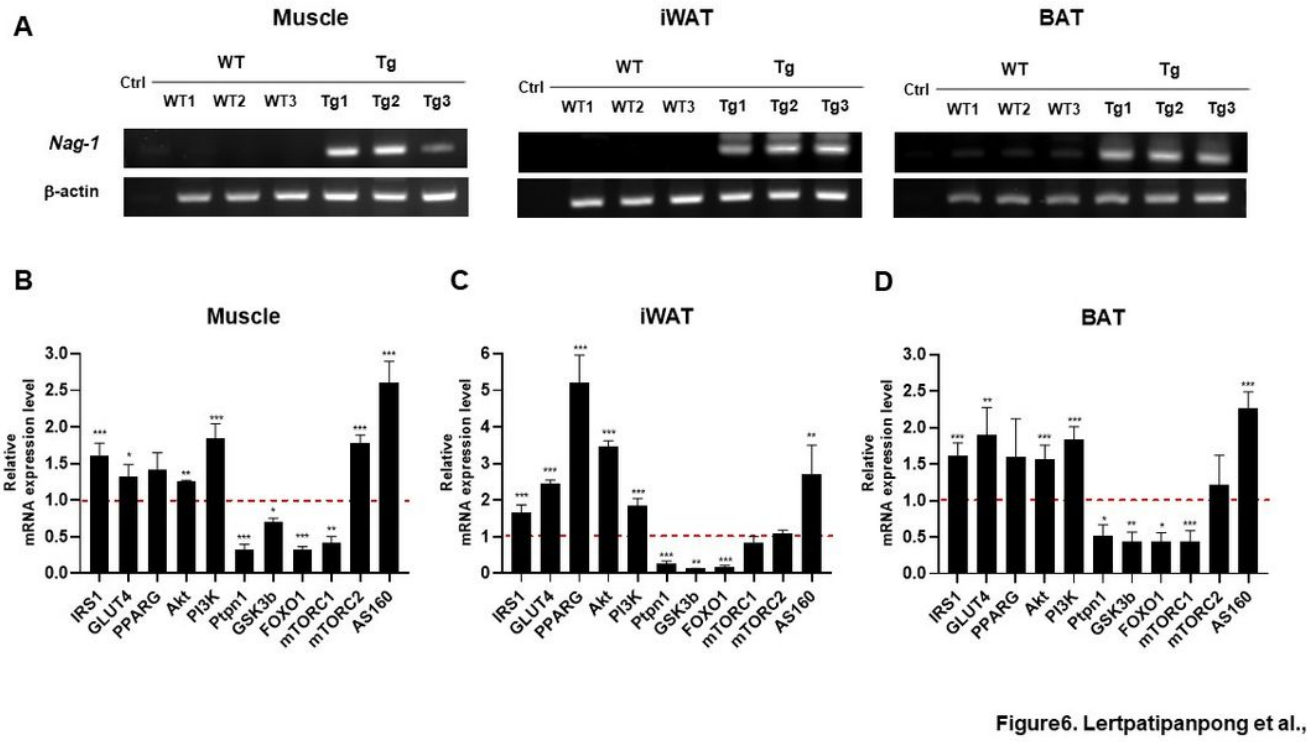

Figure6. Lertpatipanpong et al.,

Figure 6

Effect of NAG-1 on the mRNA expression level of insulin signaling pathway-related factors. (A) NAG-1 expression on muscle and adipose tissues. (B-D) The mRNA expression levels of Irs1, Glut4, Pparg, Akt, Pi3k, Ptpn1 (Pten), Gsk3b, Foxo1, Mtorc1, Mtorc2, and As160 in the (B) muscle tissue, (C) inguinal white adipose tissue, and (D) brown adipose tissue were examined using quantitative real-time polymerase chain reaction. The expression levels of target genes were normalized to those of Gapdh. Data were analyzed using the Student's t-test and are presented as mean ± standard error of mean. *p<0.05, **p<0.01, and ***p<0.001, compared with the wildtype group. (n = 3 mice per group).

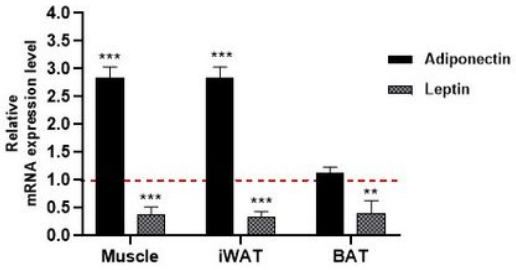

Figure7. Lertpatipanpong et al.,

Figure 7

Effect of NAG-1 on the mRNA expression level of adipocytokines. Adiponectin and leptin mRNA expression levels in the (A) muscle tissue, (B) inguinal white adipose tissue, and (C) brown adipose tissue were determined using quantitative real-time polymerase chain reaction. The expression levels of target genes were normalized with those of Gapdh. Data are presented as mean ± standard error and were analyzed using Student's t-test. *p<0.05, **p<0.01, and ***p<0.001, compared with the control group. (n = 3 mice per group).

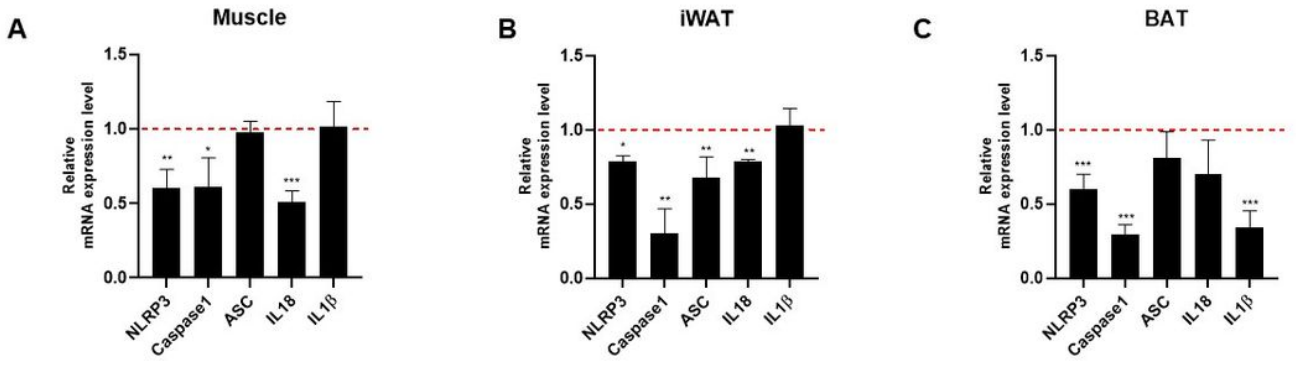

Figure8. Lertpatipanpong et al.,

Figure 8

Effect of NAG-1 on the mRNA expression level of Nlrp3 inflammasome. The mRNA expression levels of Nlrp3, Casp1, Asc, Il18, and Il1b in the (A) muscle, (B) inguinal white adipose tissue, and (C) brown adipose tissue. The expression levels of target genes were normalized to those of Gapdh. Data are presented as mean ± standard error of mean and were analyzed using Student's t-test. *p<0.05, **p<0.01, and ***p<0.001, compared with the control group (n = 3 mice per group).

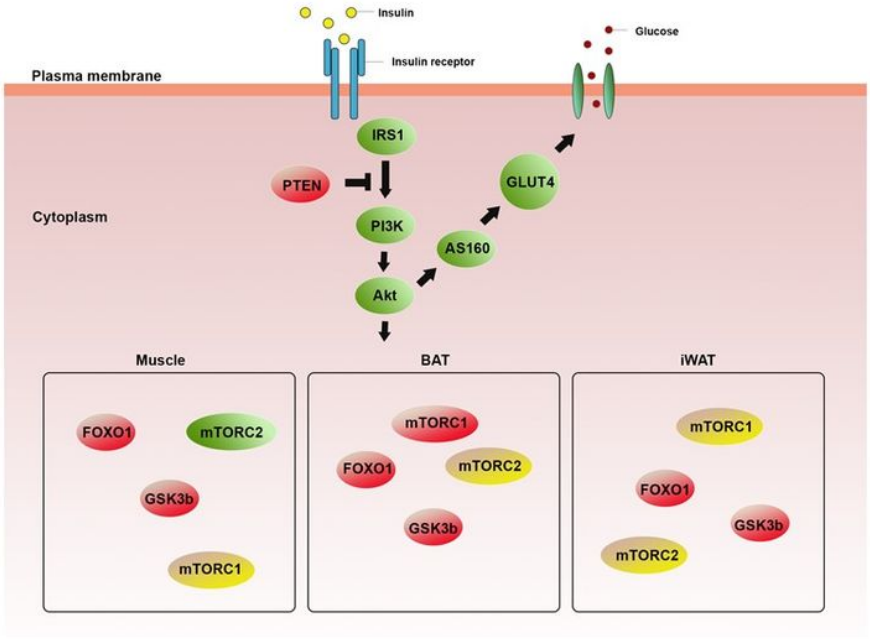

Figure9. Lertpatipanpong et al.,

Figure 9

Schematic diagram representing the effect of NAG-1 on the IRS1/PI3K/AKT signaling pathway. Green and red colors represent upregulation and downregulation, respectively.

Supplementary Files

This is a list of supplementary files associated with this preprint. Click to download.

- SupplementinformationFinal.xlsx
- Supplementaryinformation.docx.pdf